Two typical time scales of the piston effect

Pierre Carlès* and Kokou Dadzie
Laboratoire de Modélisation en Mécanique, Université Paris 6, Case 162, 4 Place Jussieu, 75252 Paris Cedex 05, France
(Received 18 August 2004; published 28 June 2005)

The existence of a fourth mode of heat transfer near the critical point, named the piston effect, has been known for more than a decade. The typical time scale of temperature relaxation due to this effect was first predicted by Onuki *et al.* [Phys. Rev A **41**, 2256 (1990)], and this author's formula has been extensively used since then to predict the thermal behavior of near-critical fluids. Recent studies, however, pointed out that the critical divergence of the bulk viscosity could have a strong influence on piston-effect-related processes. In this paper, we conduct a theoretical analysis of near-critical temperature relaxation showing that the piston effect is not governed by one (as was until now believed) but by two typical time scales. These two time scales exhibit antagonistic asymptotic behaviors as the critical point is approached: while the classical piston-effect time scale (as predicted by Onuki *et al.*) goes to zero at the critical point (critical speeding up), the second time scale (related to bulk viscosity) goes to infinity (critical slowing down). Based on this property, an alternative method for measuring near-critical bulk viscosity is proposed.

DOI: 10.1103/PhysRevE.71.066310 PACS number(s): 47.40.Dc, 47.17.+e, 05.70.Jk, 02.30.Mv

I. INTRODUCTION

Heat transfer near the liquid-vapor critical point is governed not only by diffusion, convection, and radiation, but also by a thermomechanical coupling called the piston effect. Before this effect was discovered, it had been known for some time that heat transfer close to the critical point exhibited a puzzling behavior (see, for instance, [1]), but only through Nitsche and Straub's early microgravity experiments (see, for instance, [2]) did it become clear that some unexpected heat transfer process was at work in near-critical fluid. These observations triggered a large number of studies in the late 1980s, among which are the pioneering works of Onuki *et al.* [3], Boukari *et al.* [4] and Zappoli *et al.* [5], which led to the identification of the piston effect. The dynamics of this specific-heat transfer mechanism has since been extensively studied by several groups, theoretically, numerically, or experimentally. The piston effect is described as a thermomechanical coupling accelerating the temperature relaxation close to the critical point: when a near-critical fluid confined in a closed cell is locally heated, thin thermal boundary layers form close to the heating device; owing to the extreme compressibility of near-critical fluids, the thermal boundary layers expand strongly and compress the rest of the fluid like a piston; through this isentropic compression of the bulk fluid, the average temperature in the cell rises in a fast and homogenenous way, on a much shorter time scale than through heat diffusion alone. The piston effect (PE) time scale was first predicted by Onuki *et al.* [3], its expression being as follows:

$$t_{\mathrm{PE}} = \frac{t_D}{(\gamma - 1)^2}. \qquad (1)$$

t_{PE} represents the typical time after which temperature perturbations in a closed near-critical fluid cell have almost completely relaxed by the piston effect. t_D is the typical time scale of heat diffusion in the cell (equal to L^2/D_T, with L the typical length of the fluid cell and D_T the thermal diffusivity). γ is the ratio of the heat capacities of the fluid.

Despite the good understanding of the process and of its typical time scale gained in recent years, many questions remain open. Among them is the role of bulk viscosity in temperature relaxation close to the critical point. Bulk viscosity is indeed predicted to exhibit a very strong divergence at the critical point [6,7], and this divergence will certainly have a strong influence on a thermomechanical coupling such as the piston effect. Until recently, only two contributions to this important question had been published: one by Onuki [8] and another by Carlès [9]. In his article, Onuki predicted the structure of the stress tensor in a near-critical fluid and examined its influence on relaxation processes. The predictions related to the dynamics of the piston effect in that paper were, however, made with the assumption that pressure remains homogeneous in the fluid throughout the evolution. In the other contribution by Carlès, [9], this later assumption was contradicted: the asymptotic analysis showed that a diverging bulk viscosity should have a much stronger influence on the piston effect than what Onuki predicted. Indeed, the viscous relaxation processes at hand in the heated boundary layer prevent its free expansion, thus building up pressure gradients close to the heated boundaries and weakening the piston effect. The existence of two regimes of the piston effect was predicted: a classical regime, not too close to the critical point, where Onuki's first model [3] is valid (the temperature relaxation undergoes a critical speeding up), and a viscous regime, very close to the critical point, were viscous stresses in the boundary layer oppose the piston effect (the temperature relaxation then undergoes a critical slowing down) [9]. In this second regime, the typical time scale of the piston effect becomes much different from Onuki's first formula (1), although its exact expression was not clearly identified in Carlès' work. Besides the two contributions cited above, Gillis *et al.* very recently developed a theoretical model for sound attenuation close to the critical

*Electronic address: carles@ccr.jussieu.fr

point, in which they included the effect of bulk viscosity [10]. Although this work is not explicitly related to temperature relaxation, several phenomena predicted in Gillis' model tend to confirm the existence of a second regime close to the critical point, where bulk viscosity significantly modifies the boundary layers dynamics.

In the present work, we first extend Carlès' initial model [9] to the case of a closed fluid cell whose boundaries are subjected to a prescribed and arbitrary temperature change. Based on this result, we transform the general solutions obtained under the form of Laplace transforms into the physical space of variables, and recover a general dimensional solution for the temperature relaxation in the fluid by the piston effect. This solution, generalized to an arbitrary set of boundary conditions, shows that the piston effect is not governed by one time scale (as believed until now) but by two: Onuki's classical piston effect time scale (1) and a viscous time scale whose expression is predicted as a function of the fluid's properties (and, in particular, of the bulk viscosity). The identification of a new and so far unsuspected time scale in the piston effect process leads to the definition of an original experimental strategy aimed at measuring the bulk viscosity close to the critical point.

In Sec. II, the problem under study is presented, followed by Sec. III, where the asymptotic method of resolution is described. Section IV is then devoted to the analysis of the obtained results in terms of the physics of the piston effect, and the new experimental setup for measuring the near-critical bulk viscosity is presented in Sec. V.

II. PROBLEM UNDER STUDY

A. Description of the system

We consider here a supercritical fluid confined between two infinite walls, separated by a distance L. The limitation to a one-dimensional (1D) geometry is in no way restrictive, since previous analysis showed that 1D models of the piston effect could easily be extended to complex 3D geometries using the right similarity coefficients [11,12]. The fluid is initially at rest and thermal equilibrium, at critical density ρ_c (a condition frequently fulfilled in classical experiments on the critical point, but in no way necessary for the present study), and at a temperature T_i slightly above the critical temperature T_c (hence, the initial pressure P_i is slightly above the critical pressure P_c too). Let us define ΔT as the initial reduced temperature,

$$\Delta T = \frac{T_i - T_c}{T_c}. \tag{2}$$

No convection is considered here, which means that the fluid cell is either in microgravity conditions or that all boundary heatings take place from above (in which case, the effect of density stratification may be considered too, see [13]). At a given time $t=0$, a time-dependent temperature is imposed at the left wall ($x=0$), while the right wall ($x=L$) is thermally insulated. This setup is represented in Fig. 1.

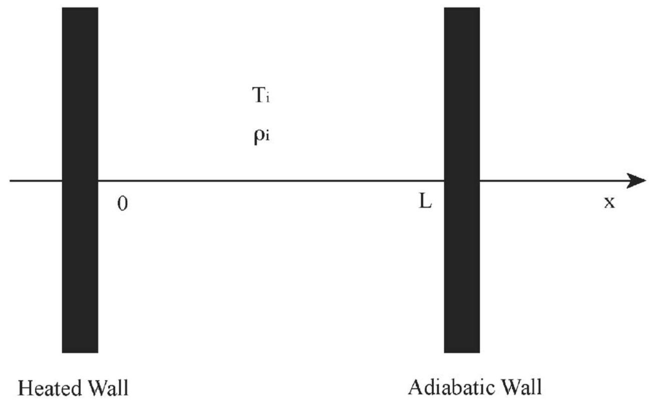

FIG. 1. System under study.

B. Modeling of the problem

Supercritical fluids exhibit singular properties at the critical point. In particular, it is known that isothermal compressibility, heat capacities, and thermal conductivity go to infinity, while heat diffusivity, sound velocity, and surface tension go to zero. These critical divergences follow power laws with universal exponents for all critical systems of the same universality class [14]. In order to simplify the presentation of the analytical calculation, the following power laws have been considered along the critical isochore:

$$C_v = C_{v_0}\Delta T^{-\alpha},$$

$$\lambda = \lambda_0 \Delta T^{-x_\lambda},$$

$$\left(\frac{\partial \rho}{\partial P}\right)_T = \Gamma_0 \Delta T^{-\gamma},$$

$$C_s = C_0 \Delta T^{\alpha/2}, \tag{3}$$

where C_v is the heat capacity at constant volume, λ is the thermal conductivity, and C_s is the sound velocity. The quantities with the subscript ($_0$) are the prefactors, and the exponents applied to ΔT are the universal critical exponents (with $\alpha \approx 0.11$, $x_\lambda \approx 0.64$, and $\gamma \approx 1.24$). Note that this representation of the fluid's thermophysical properties is rigorously valid only on the critical isochore and in the domain where critical divergences dominate the nonuniversal behavior of the fluid. But as will be seen later, the results obtained through the asymptotic analysis described below can straightforwardly be generalized to any set of diverging properties, provided the global hierarchy of the different asymptotic divergences is kept the same as above. In other words, all the results presented here will be directly applicable to fluid cells slightly off-critical in terms of density, or to thermodynamic states where the regular contribution to thermophysical properties is still significant. In the same way as above, the divergence of the bulk viscosity is simply written as

$$\frac{\frac{4}{3}\eta_s+\eta_B}{\rho_c}=\Theta_0\Delta T^{-x_{\eta_B}}, \tag{4}$$

where η_s is the shear viscosity, η_B is the bulk viscosity with Θ_0 its prefactor, and x_{η_B} is its critical exponent. x_{η_B} is thought to be about 1.94 [7,15,8], which means that the critical divergence of the bulk viscosity is certainly the strongest one of all thermophysical properties. Note that the shear viscosity η_s exhibits a very slow divergence at the critical point, totally negligible compared to that of the bulk viscosity. In the above definitions, the value of each property is defined as a function of the initial reduced temperature. In other words, it will be considered constant throughout the evolution of the fluid. This choice implies a limitation on the amplitude of the temperature heating law: the boundary heating must be small enough to be able to consider that the fluid's properties are not affected by the temperature change.

The fluid motion is represented by the one-dimensional unsteady Navier-Stokes equations, to which are added the equation of energy and an arbitrary equation of state. The following dimensionless quantities are defined:

$$T^*=\frac{T}{T_c},\quad P^*=\frac{P}{P_c},\quad \rho^*=\frac{\rho}{\rho_c},$$

$$U^*=\frac{U}{C_s},\quad x^*=\frac{x}{L},\quad t^*=\frac{tC_s}{L}, \tag{5}$$

where T, P, and ρ are the thermodynamic coordinates, U is the macroscopic fluid's velocity, and x and t are the space and time variables. In the above formulas, stars (*) denote dimensionless quantities. The dimensionless equations of the problem are then (the stars have been omitted for the sake of readability)

$$\rho_t+(\rho U)_x=0, \tag{6a}$$

$$\rho U_t+\rho UU_x=-A\Delta T^{-\alpha}P_x+\epsilon\eta_0\Delta T^{(-\alpha/2)-x_{\eta_\beta}}U_{xx}, \tag{6b}$$

$$\rho T_t+\rho UT_x=-B\Delta T^{\alpha}TU_x+\epsilon\frac{\gamma_0}{Pr_0}\Delta T^{(\alpha/2)-x_\lambda}T_{xx}+\epsilon\eta_0B^2\Delta T^{(3/2)\alpha-x_{\eta_\beta}}U_x^2, \tag{6c}$$

$$\delta P=C\delta T+D\delta T^{\gamma}\delta\rho, \tag{6d}$$

where the following coefficients are dimensionless quantities of order 1:

$$A=\frac{P_c\rho_cC_{v_0}}{T_c}\left(\frac{\partial T}{\partial P}\right)^2_\rho,\quad B=\frac{1}{\rho_cC_{v_0}}\left(\frac{\partial P}{\partial T}\right)_\rho,$$

$$C=\frac{T_c}{P_c}\left(\frac{\partial P}{\partial T}\right)_\rho,\quad D=\frac{\rho_c}{P_c\Gamma_0},$$

$$\frac{\gamma_0}{Pr_0}=\frac{\lambda_0}{\eta_{s_0}C_{v_0}},\quad \eta_0=\frac{\rho_c\theta_0}{\eta_{s_0}}. \tag{7}$$

Note that the product ABC is equal to 1. Equation (6a) is the continuity equation, Eq. (6b) is the momentum equation, Eq. (6c) is the energy equation, and Eq. (6d) is an arbitrary equation of state in differential form. In the above equations, two dimensionless small parameters appear: ΔT [already defined in Eq. (2)] and ϵ, defined as

$$\epsilon=\frac{\eta_{s_0}}{\rho_cLC_0}. \tag{8}$$

With this definition, ϵ appears as the inverse of a reference acoustic Reynolds number. To the above system are added the following boundary and initial conditions. A time-dependent temperature is imposed at the left wall ($x=0$),

$$T(x=0,t)=T_i+T_{wall}(t), \tag{9}$$

which can be written in dimensionless form as

$$T^*(x^*=0,t^*)=1+\Delta T+\theta T^*_w(t^*), \tag{10}$$

where $\theta=(1/T_c)\max|T_{wall}(t)|$. Through this definition, T^*_w is a function of time varying from 0 to 1 (or -1 in the case of a cooling), while θ is the order function representing the dimensionless amplitude of the wall temperature perturbation. In order to ensure that the properties of the fluid are not significantly modified by the local heating, one has to impose $\theta\ll\Delta T$.

The right wall is chosen to be adiabatic, hence

$$T^*_{x^*}(x^*=1,t^*)=0. \tag{11}$$

Both walls are solid, so

$$U^*(x^*=0,t^*)=U^*(x^*=1,t^*)=0. \tag{12}$$

The initial conditions are then

$$T^*(x^*,t^*=0)=1+\Delta T,\quad \rho^*(x^*,t^*=0)=1,$$

$$P^*(x^*,t^*=0)=P^*_i=1+\Delta P,\quad U^*(x^*,t^*=0)=0. \tag{13}$$

The above system of equations with the related boundary and initial conditions is too complex to solve in exact form. However, the existence of small parameters linked to the critical divergences suggests an asymptotic approach. In the next section, an asymptotic analysis of the system is presented.

III. ASYMPTOTIC ANALYSIS OF THE SYSTEM

In system (6a)–(6d), ϵ and ΔT are both much smaller than unity. For instance, in the case of a 1-mm cell filled with ^{3}He, $\epsilon=4.5\times10^{-7}$, while ΔT can be arbitrarily small, depending on the initial temperature. For the sake of the asymptotic analysis, both of these parameters will be considered as going to zero.

In cases where two asymptotically small parameters are present, asymptotic analyses must be conducted with great caution. Indeed, the final result of the asymptotic process can be dependent upon the relative rate at which the two parameters go to zero. When such a phenomenon is observed, the system is said to be singular in the space of parameters. An asymptotic analysis of system (6a)–(6d) was already conducted in [9] (for a less general set of boundary conditions), which led to the identification of such a singularity. In other words, the reduced system of equations obtained from Eqs. (6a)–(6d) by making first ϵ and then ΔT go to zero is different from the one obtained by making first ΔT and then ϵ go to zero. This problem was handled in [9] by constructing an intermediate system through which these two extreme cases could be matched. It was shown that such an intermediate system could be obtained by making ϵ and ΔT go to zero with ζ fixed, where

$$\zeta = \frac{\Delta T}{\epsilon^{2/\chi}} \tag{14}$$

with $\chi = 2\gamma + x_\lambda + x_{\eta_B} - 2\alpha$. The parameter ζ appears naturally as a result of the asymptotic analysis process, but it has a physical meaning which will be discussed in the next section. The system obtained with ζ fixed is called the inner description. It is more general than the two systems obtained by making first ϵ and then ΔT go to zero or first ΔT and then ϵ. Each of these systems (called the outer descriptions) can be deduced from the inner description by making ζ go to infinity or to zero, after the asymptotic series have been obtained. Two different regimes of the piston effect were thus identified in [9]: one, for $\zeta \gg 1$ (i.e., not too close to the critical point), is the classical regime of the piston effect, already presented in [16,11,12] (and equivalent to Onuki's initial model [3]); the other one, for $\zeta \ll 1$ (i.e., very close to the critical point), is a regime where viscous stresses dominate the relaxation dynamics, and was thus named the viscous regime of the piston effect.

In the present work, we try to characterize the dynamics of temperature relaxation through these three regimes (classical, intermediate, and viscous), and in particular to identify an explicit form of the typical time scales involved in this process (a general result not obtained in our previous work [9]). As said above, the system obtained for ζ fixed (the inner description) is the most general system which can be obtained through the asymptotic limits of ΔT and ϵ. In the present study, Eqs. (6a)–(6d) are thus expanded for the following conditions:

$$\Delta T \to 0,$$

$$\epsilon \to 0,$$

$$\zeta = O(1). \tag{15}$$

As can be seen in Eq. (6c), making ΔT and ϵ go to zero for fixed x^* and t^* leads to the disappearance of the heat diffusion term in the equation of energy. In other words, the system becomes adiabatic, which prevents the wall heating from having any thermal effect on the fluid. This is due to another type of singularity: a spatial singularity. Indeed, the diffusion term in Eq. (6c) is negligible everywhere in the fluid except very close to the heated wall, where strong temperature gradients counterbalance the weak heat diffusivity. The effect of heat diffusion is thus not absent from the fluid, but simply limited to a very thin boundary layer close to the heated wall. This layer is asymptotically thin (in terms of ΔT and ϵ), so that it can only be observed through a change of variable in which x^* is replaced by z^*, with

$$z^* = \frac{x^*}{\delta} \tag{16}$$

and

$$\delta = \delta(\Delta T, \epsilon) = o(1). \tag{17}$$

Two systems are consequently necessary to describe the behavior of the whole fluid: an outer expansion conducted for $[\Delta T \to 0,\ \epsilon \to 0,\ \zeta = O(1)]$ with x^* fixed, which describes the dynamics of the bulk fluid, and an inner expansion (or boundary layer expansion) conducted for $[\Delta T \to 0,\ \epsilon \to 0,\ \zeta = O(1)]$ with z^* fixed, which describes the boundary layer dynamics. The definition of δ as a function of ΔT and ϵ is obtained by ensuring that the term representing thermal diffusion in Eq. (6c) survives the asymptotic process in the boundary layer expansion. The matching between the two systems is then made using the method of matched asymptotic expansions [17]. Note that at the begining of the asymptotic analysis, the typical time scale on which the system must be expanded (i.e., the typical time scale of the piston effect) is unknown: it is defined through the dimensionless time variable τ^*, which is related to t^* through

$$\tau^* = e t^*, \tag{18}$$

where

$$e = e(\Delta T, \epsilon) = o(1). \tag{19}$$

The characterization of e is obtained by ensuring that the temperature perturbations in the boundary layer and in the bulk fluid are of the same order of magnitude (in other words, by ensuring that on the time variable τ^*, the piston effect has already significantly thermalized the fluid cell). As will be seen in the result of the asymptotic analysis, e is such that the typical time scale of the piston effect remains longer than the acoustic one and shorter than the diffusive one throughout the parametric domain of interest here. The propagation of thermoacoustic waves in the cell will thus be filtered in the present work, with only their average effect on relaxation processes being considered.

Once all the different variables and systems are asymptotically constructed, a set of solutions for the temperature relaxation can be calculated, based on the chosen boundary and initial conditions (10)–(13). The whole asymptotic process and the related calculations are described in the Appendix.

IV. RESULTS AND DISCUSSION

A. Bulk temperature solution: The two time scales of the piston effect

The asymptotic process described above leads to a set of first-order uniformly valid solutions for the temperature, density, pressure, and velocity profiles in the fluid cell, at all times and for all positions in the cell. These solutions can be applied to any initial reduced temperature, since the inner description on which they are based [i.e., the expansion at $\zeta = O(1)$] is the most general expansion of the system under study (it implicitly contains all the different regimes of the piston effect). An interesting particular solution is the one governing the evolution of the bulk temperature, i.e., the temperature of the fluid far from the heated walls (which is uniform in the whole fluid cell apart from the boundary layers). This temperature solution is a direct measure of the temperature relaxation in the fluid by the piston effect. Let us denote the bulk temperature variation as T_b, and the heated wall temperature variation as T_w [see Eq. (10)]. When translated into dimensional variables, the asymptotic solution becomes (under the form of a Laplace transform)

$$T_b(s) = T_w(s) \,. \frac{1}{1 + \sqrt{\left(\frac{DPr_0 L}{BC\gamma_0 C_s \epsilon}\Delta T^{\gamma + x_\lambda - (3/2)\alpha}\right)s + \left(\frac{\eta_0 Pr_0 L^2}{\gamma_0 C_s^2}\Delta T^{x_\lambda - \alpha - x_{\eta_\beta}}\right)s^2}}, \tag{20}$$

where s is the Laplace complex parameter (whose dimension is the inverse of a time). The above solution is of course based on the specific form of transport coefficients presented in Eq. (3). Using these last definitions, it is possible to relate the coefficients in Eq. (20) to the thermophysical properties of the fluid in an explicit manner. The bulk temperature solution then becomes

$$T_b(s) = T_w(s) \frac{1}{1 + \sqrt{\frac{s}{\Omega_c} + \frac{s^2}{\Omega_v^2}}}, \tag{21}$$

where

$$\Omega_c = -\frac{T_c \lambda}{\rho_c^3 L^2 C_v^2}\left(\frac{\partial \rho}{\partial T}\right)_P \left(\frac{\partial P}{\partial T}\right)_\rho \tag{22}$$

and

$$\Omega_v^2 = \frac{T_c \lambda}{\rho_c^2 L^2 C_v^2\left(\eta_B + \frac{4}{3}\eta_s\right)}\left(\frac{\partial P}{\partial T}\right)_\rho^2. \tag{23}$$

The above solution (21) generalizes Eq. (20) for thermophysical properties of more general expressions than those considered in Eq. (3). Indeed, the asymptotic expansion as detailed in the Appendix remains valid for all sets of properties with equivalent asymptotic relationships to the one considered here. In other words, the solutions obtained here are not limited to the specific forms of thermophysical properties presented in Eq. (3), which were chosen only in order to simplify the exposition of the calculation.

Expression (21) shows that the Laplace transform of the bulk temperature variation is obtained as the product of the Laplace transform of the temperature variation at the heated wall with a characteristic function of the system. When the inverse Laplace transform of this expression is calculated, one obtains

$$T_b(t) = T_w(t) * i(t), \tag{24}$$

where $*$ represents the convolution product, and

$$i(t) = \mathcal{L}^{-1}\left[\frac{1}{1 + \sqrt{\frac{s}{\Omega_c} + \frac{s^2}{\Omega_v^2}}}\right]. \tag{25}$$

Using the classical terminology of signal theory, $i(t)$ can be called the impulse response of the system, its Laplace transform being the system's transfer function. $i(t)$ is independent of the heating law $T_w(t)$: it thus characterizes the thermal response of the supercritical fluid cell itself. One can observe that $i(t)$ and its associated transfer function depend only on two typical pulsations, Ω_c and Ω_v. These quantities are the inverse of two typical times, which can be expressed in an explicit way,

$$\frac{1}{\Omega_c} = t_{\mathrm{PE}} = \frac{t_D}{(\gamma - 1)^2}, \tag{26}$$

$$\frac{1}{\Omega_v} = t_v = \sqrt{t_{\mathrm{PE}}\left(\eta_B + \tfrac{4}{3}\eta_s\right)\kappa_T} \simeq \sqrt{t_{\mathrm{PE}}\eta_B \kappa_T} \tag{27}$$

with κ_T the isothermal compressibility,

$$\kappa_T = \frac{1}{\rho}\left(\frac{\partial \rho}{\partial P}\right)_T. \tag{28}$$

The above expressions lead to the first conclusion of the present study: the piston effect's typical response is not governed by one typical time (as was believed until now), but by two: one of them, t_{PE} (26), is the classical piston effect typical time, first identified by Onuki *et al.* [3]. The other one, t_v (27), is the viscous typical time: it characterizes the time delay that viscous stresses impose to the free thermal expansion of the boundary layer. When this delay is much smaller than the piston effect time scale itself, viscosity has almost no effect. When it is longer, on the contrary, it becomes the limiting factor of the thermal relaxation. The thermal response of the fluid is thus conditioned by the longer of the two characteristic times t_{PE} and t_v.

Let us examine the evolution of t_{PE} and t_v with the initial reduced temperature ΔT,

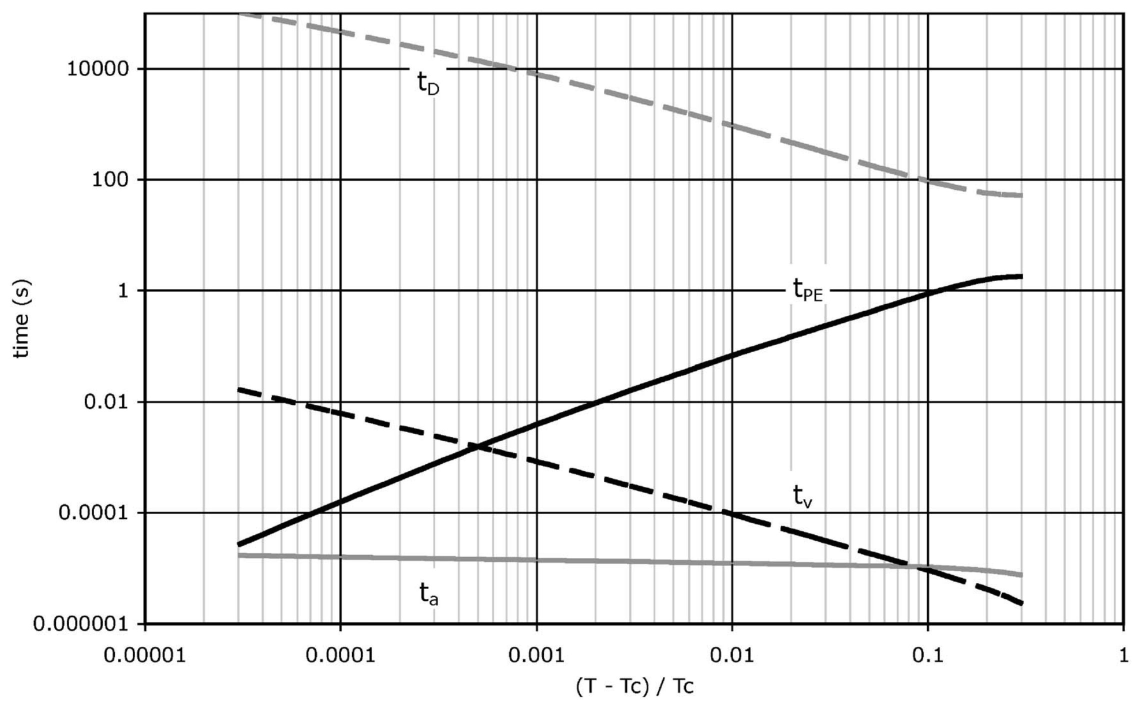

FIG. 2. Classical time scale (dark full line) and viscous time scale (dark dotted line) of the piston effect, compared with the typical time scales of heat diffusion (gray dotted line) and of acoustic properties.

$$t_{\mathrm{PE}} \propto \Delta T^{\gamma-2\alpha+x_\lambda} \approx \Delta T^{1.66}, \tag{29}$$

$$t_v \propto \Delta T^{(1/2)(x_\lambda - x_{\eta_B})-\alpha} \approx \Delta T^{-0.74}. \tag{30}$$

The above scaling relations show that t_{PE}, the classical piston effect time scale, goes to zero at the critical point: this illustrates the well-known phenomenon of the critical speeding up. But at the same time, t_v goes to infinity at the critical point: when t_v becomes larger than t_{PE}, a critical slowing down should occur. This observation was first made in [9], although not quantified in a general manner. The expressions obtained for t_{PE} and t_v and their critical behavior now enable us to identify more clearly the physical meaning of the inner parameter ζ. Indeed, one has

$$\zeta \propto \left(\frac{t_{\mathrm{PE}}}{t_v}\frac{1}{\epsilon}\right)^{2/\chi}. \tag{31}$$

Hence, ζ, which came naturally out of the asymptotic process, is found to be proportional (to a certain power) to the ratio of the two typical times of the piston effect. In Fig. 2, the different typical time scales of the problem have been drawn as functions of ΔT for a 1-mm cell filled with ^{3}He: the classical time of the piston effect t_{PE}, the viscous time of the piston effect t_v, the typical time of heat diffusion $t_D = L^2\rho_c C_p/\lambda$, and the typical acoustic time $t_a = L/C_s$. These typical times have been drawn using the full expressions of the thermophysical properties of ^{3}He [not restricted to the universal component as in Eq. (3)], as calculated by a model provided by Fang Zhong from JPL [18].

The crossover between a regime of critical speeding up and a regime of critical slowing down can be clearly observed: as long as ΔT is larger than 5×10^{-4} (i.e., $t_{\mathrm{PE}} > t_v$), the temperature relaxation is dominated by t_{PE} and thus undergoes a critical speeding up: the fluid cell is in the classical regime of the piston effect; when ΔT becomes smaller than 5×10^{-4}, on the contrary (i.e., $t_{\mathrm{PE}} < t_v$), the relaxation is governed by t_v, which is longer and longer as the critical point is approached: the fluid cell enters the viscous regime of the piston effect, where a critical slowing down occurs. Note that Fig. 2 has been drawn using an estimated value of η_0, based on Onuki's expression for the zero-frequency value of the bulk viscosity [8] ($\eta_0 = 0.0235$). The physical interpretation of the origin of this second regime lies in the strong divergence of the bulk viscosity: when bulk viscosity becomes larger and larger, viscous stresses progressively tend to oppose the free thermal expansion of the boundary layers, which weakens the piston effect; in the viscous regime, the divergence of the bulk viscosity becomes strong enough to overcome the divergence of the isothermal compressibility, so that the viscous weakening becomes more and more pronounced: the temperature relaxation slows down at the critical point.

B. The classical regime of the piston effect

As said above, the classical regime of the piston effect is observed when t_{PE} is much larger than t_v. In this case, one has (except for very early times, characterized by $|s| \gg \Omega_v^2/\Omega_c$)

$$\left|\frac{s}{\Omega_c}\right| \gg \left|\frac{s^2}{\Omega_v^2}\right| \tag{32}$$

so that $i(t)$ becomes

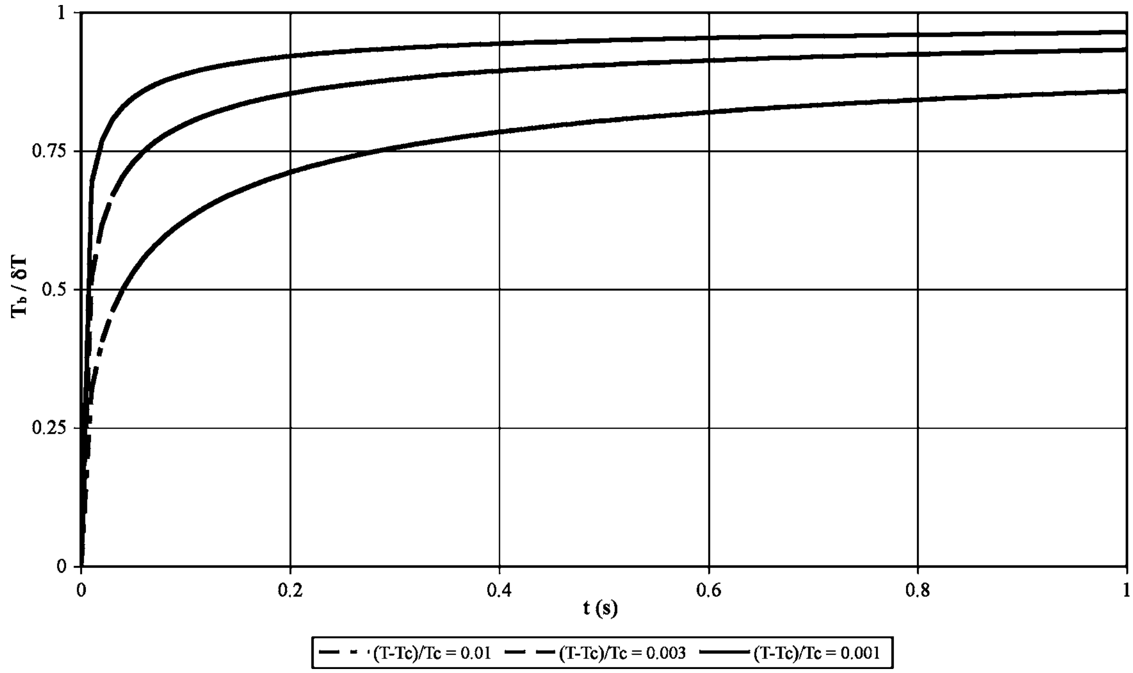

FIG. 3. Time evolution of the bulk temperature after a quench of the fluid cell of amplitude δT, for different reduced temperatures in the classical regime of the piston effect (the fluid cell is 1 mm long and filled with ^{3}He).

$$i(t) \approx \mathcal{L}^{-1}\left(\frac{1}{1+\sqrt{\frac{s}{\Omega_c}}}\right) = \sqrt{\frac{\Omega_c}{\pi t}} - \Omega_c \exp(\Omega_c t) \mathrm{erf}\, c(\sqrt{\Omega_c t}). \tag{33}$$

The condition $|s| \gg \Omega_v^2/\Omega_c$ translates in time to $t \ll t_v^2/t_{\mathrm{PE}}$. For instance, in ^{3}He at $\Delta T = 0.01$, the above simplification is thus valid for values of the time t larger than 0.1 μs. Given the expression of the impulse response $i(t)$, it is easy to find the temperature response of the bulk fluid to any wall temperature law using relation (24). It can be easily checked that the obtained result is equivalent to the thermal response predicted by Onuki *et al.* in [3], by Carlès in [11], and by Zappoli and Carlès in [16] for different heating laws. The classical results obtained so far on the piston effect dynamics by several groups are thus recovered as particular cases of the present theory. A temporal evolution of the bulk temperature $T_b(t)$ has been drawn in Fig. 3 for a 1-mm cell filled with ^{3}He, subjected to a sudden temperature quench of amplitude δT. The different curves relate to different initial reduced temperatures ΔT, all chosen above 5×10^{-4} (that is, in the classical regime of the piston effect). The critical speeding up of temperature relaxation is clearly visible.

C. The viscous regime of the piston effect

When t_v is much larger than t_{PE} (in contrast to the previous case), then the piston effect is in the so-called viscous regime. As said above, this regime is characterized by the fact that strong viscous stresses build up in the thermal boundary layers, opposing their free expansion. The piston effect is consequently weakened and this weakening is more and more pronounced as the critical point is approached due to the strong divergence of the bulk viscosity. The general form of the impulse response $i(t)$ can then be simplified into (except for very late times, characterized by $|s| \ll \Omega_v^2/\Omega_c$)

$$i(t) \approx \mathcal{L}^{-1}\left(\frac{1}{1+\frac{s}{\Omega_v}}\right) = \Omega_v \exp(-\Omega_v t). \tag{34}$$

For instance, in ^{3}He at $\Delta T = 3 \times 10^{-5}$, the above simplification is valid for values of the time t smaller than 10 s. The above expression for $i(t)$ is very interesting, as it has an explicit meaning in the framework of signal theory: it is the typical impulse response of a first-order low-pass filter of cutoff pulsation Ω_v. Through Eq. (24), the relationship between the wall and bulk temperatures can consequently be summarized in the following way: in the viscous regime of the piston effect, the bulk temperature follows the wall temperature filtered through a first-order low-pass filter. In other words, harmonic components of the wall temperature law of frequencies smaller than the cutoff frequency will be reproduced exactly in the bulk fluid, while components of higher frequencies will be strongly attenuated. Note that the cutoff pulsation Ω_v goes to zero at the critical point [see Eq. (30)]. This property explains the critical slowing down predicted close to the critical point: the bulk thermal response can only follow slower and slower temperature changes at the wall. Let us now examine two particular heating laws and the associated bulk temperature evolutions.

First, let us consider a temperature quench at the wall, like the one used to draw Fig. 3,

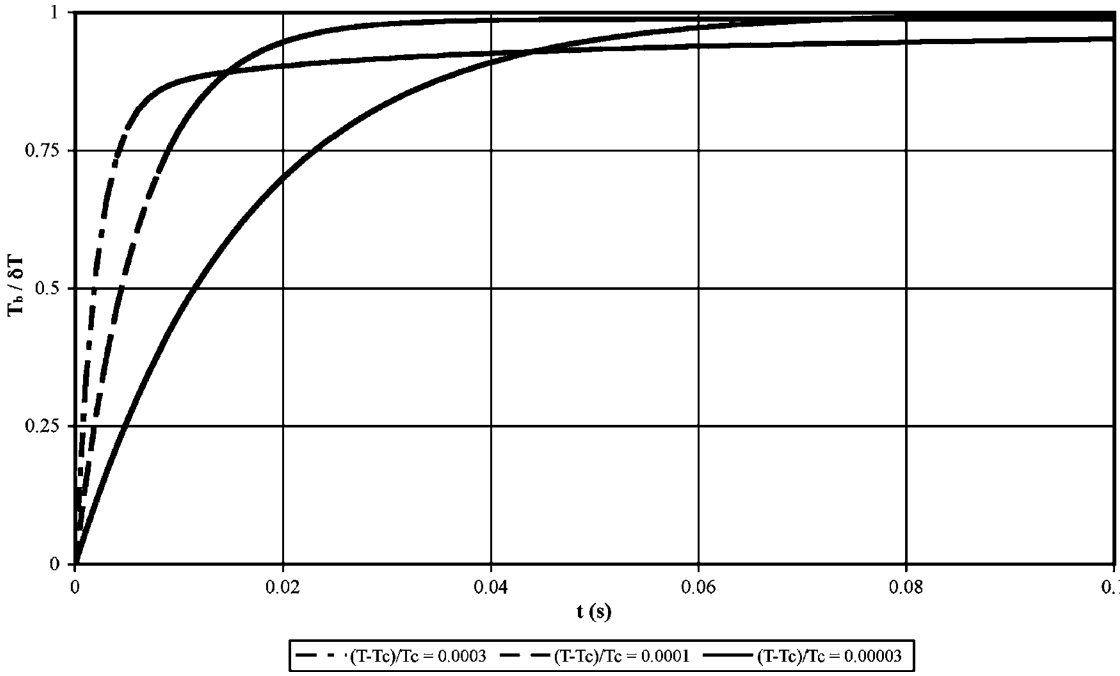

FIG. 4. Time evolution of the bulk temperature after a quench of the fluid cell of amplitude δT, for different reduced temperatures in the viscous regime of the piston effect (the fluid cell is 1 mm long and filled with ^{3}He).

$$T_{w_1}(t) = \delta T\,\mathcal{H}(t), \tag{35}$$

where $\mathcal{H}(t)$ is the Heavyside function and δT the amplitude of the temperature increase. Then the bulk temperature increase $T_{b_1}(t)$ is

$$T_{b_1}(t) = \delta T[1 - \exp(-\Omega_v t)]. \tag{36}$$

The bulk temperature response to the quench has been plotted in Fig. 4, calculated for a 1-mm cell filled with ^{3}He. As in Fig. 3, the different curves relate to different initial reduced temperatures ΔT, all chosen below 5×10^{-4} (that is, in the viscous regime of the piston effect). The critical slowing down of temperature relaxation is clearly visible, as opposed to the critical speeding up observed in Fig. 3. A peculiar observation can, however, be made about Fig. 4: although at early times, a critical slowing down of the relaxation indeed occurs, a critical speeding up is recovered at late times. It is at present difficult to give a clear interpretation of this phenomenon, but it can be understood if the viscous time scale t_v is indeed viewed as a delay: such a finite delay may have a strong influence on early-time behavior and a negligible one on late-time behavior (thus explaining that the late-time behavior follows the classical nonviscous dependence on reduced temperature).

Let us now consider an oscillating temperature variation at the wall, of amplitude δT and pulsation ω,

$$T_{w_2}(t) = \delta T \sin(\omega t). \tag{37}$$

The bulk temperature variation is then

$$T_{b_2}(t) = \delta T \frac{\Omega_v}{\sqrt{\Omega_v^2 + \omega^2}} \sin(\omega t - \phi) \tag{38}$$

with $\tan(\phi) = \omega/\Omega_v$. The above expression is particularly interesting, as it clearly stresses how the viscosity-dominated piston effect filters the boundary temperature evolution: when $\omega \ll \Omega_v$, T_{b_2} almost follows T_{w_2} exactly: the bulk temperature variation reproduces the wall temperature variation; when $\omega \gg \Omega_v$, on the contrary, the amplitude of the bulk temperature variation decreases strongly with ω, like ω^{-1}. At the same time, the phase lag between the wall and the bulk temperature goes from 0 (for small frequencies) to $-\pi/2$ (for large frequencies). This behavior is illustrated in Fig. 5, where the amplitude ratio between $T_{b_2}(t)$ and $T_{w_2}(t)$ is plotted as well as the phase lag between them.

D. A new way of measuring near-critical bulk viscosity

Expression (38) and Fig. 5 suggest a new way of measuring near-critical bulk viscosity. Indeed, Ω_v is an explicit function of the bulk viscosity η_B [see Eq. (23)]. In other words, if the other properties of the fluid are known with enough precision, then an indirect measure of the bulk viscosity could be deduced from the characterization of the cutoff pulsation of the piston effect in the viscous regime. Such a characterization could be done as follows.

A closed fluid cell would have to be constructed, under the form of a small gap between two large horizontal plates of copper, the gap being filled with a near-critical fluid at critical density. The top and bottom copper walls would then have to be heated and cooled in a periodic way, so as to impose a small-amplitude monochromatic oscillation of the temperature at the interfaces between the two walls of copper

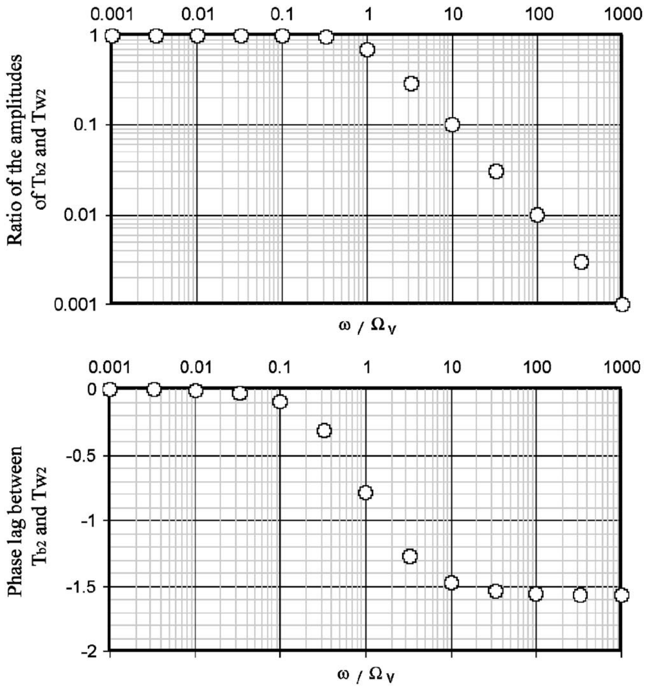

FIG. 5. Ratio of the amplitudes and phase lag between the wall and the bulk temperature oscillations in the viscous regime of the piston effect; the fluid cell is 1 mm long, filled with ^{3}He, and subjected to a boundary temperature oscillation of pulsation ω.

and the fluid. The only internal measurement needed would then be a time-resolved measurement of the wall temperatures and of the temperature in the middle plane of the fluid layer. The first temperatures (which should be equal) would be equivalent to $T_w(t)$ in our model, while the middle-plane temperature would be equivalent to $T_b(t)$ in our model. Then, by sweeping the frequency of the oscillatory heating, one would only need to measure for each frequency the ratio of the amplitudes of $T_w(t)$ and $T_b(t)$ as well as their phase lag, and identify Ω_v through these measurements (something which could easily be done on plots such as the ones in Fig. 5). Knowing Ω_v would directly yield the value of η_B, the bulk viscosity. Note that instead of being confined in between two conducting walls of imposed time-varying temperatures, the fluid layer could be confined between one heated wall and one adiabatic wall. Then $T_w(t)$ would be measured on the heated wall and $T_b(t)$ on the adiabatic wall (a solution which would allow us to avoid putting sensors inside the fluid).

A similar experimental strategy, based on a periodic boundary heating, was proposed by Zhong *et al.* [19] based on a suggestion by Onuki [8]. In these authors' reference, however, two elements made this strategy inapplicable to measuring the bulk viscosity: first, the authors evaluated the possibility of measuring the bulk viscosity through a measure of the bulk density response to a boundary oscillatory heating (a less sensitive diagnostic than temperature); besides, they relied for their estimation of the amplitude of the effect on Onuki's model [8], which omitted the effect of the bulk viscosity on pressure in the boundary layer (as discussed before) and thus underestimated the global influence of this property on relaxation processes. The experimental strategy we present here is thus significantly different from the one described in [19], and based (in our view) on a more precise understanding of dynamic processes close to the critical point.

Of course, only the rough principle of the experiment has been described here. In order for such a principle to be applicable in practice, a detailed feasability analysis should be conducted (something which is beyond the scope of this paper). Apart from the usual problems encountered in near-critical experiments (finite-size effects, gravity effects, precision of the thermal control, etc.), two other issues will have to be considered: (i) the fact that the measure of the bulk viscosity will only be indirect; (ii) the frequency dependence of the bulk viscosity close to the critical point. The first issue is linked to the proposed experimental procedure: the bulk viscosity will not be measured directly, but will be obtained from a calculation based on the measurement of a cutoff pulsation. Consequently, this indirect calculation of η_B from the cutoff pulsation Ω_v will only be as precise as the prediction of the other properties on which Ω_v depends (among which are the thermal diffusivity and the heat capacities). This condition can put a limit on the precision accessible through the proposed strategy. The second issue is related to the viscoelastic behavior of near-critical fluids (see, for instance, Onuki *et al.* [8] and Berg *et al.* [20]): close to the critical point, the frequency domain where viscosity is frequency-dependent becomes larger and larger. Consequently, frequency-dependent phenomena may appear even for frequencies as small as $\Omega_v/2\pi$. This consideration illustrates the need to extend the present theory to include frequency-dependent thermophysical properties, if one is to consider building an experiment like the one described here. Such an extension is beyond the scope of this paper. Only a careful analysis of the two issues cited above will tell whether the principle presented here will improve the measurement of bulk viscosity near the critical point (as compared to the more classical use of sound attenuation, like in Zhong *et al.* [19] and Gillis *et al.* [10]).

However, even if the estimated precision proves to be too bad for a practical measurement to be conducted, the experiment described above could nonetheless lead to an interesting result: the experimental identification of the second regime of the piston effect, never made until now even in recent experiments. This perspective may make the construction of such an experiment worth the effort. We are presently conducting a first dimensional analysis in this direction, in collaboration with the Jet Propulsion Laboratory (NASA / California Institute of Technology, USA) [21].

V. CONCLUSION

In the present work, techniques of asymptotic analysis have been applied to the problem of heat and mass transfer in a boundary-heated cell filled with a near-critical fluid. Taking into account the critical divergence of the bulk viscosity, a general set of solutions has been found which describes the temperature, pressure, density, and velocity profiles in the fluid cell when subjected to an arbitrary boundary temperature change. Although the temperature relaxation in the fluid cell is governed by the now classical phenomenon of the piston effect for all initial conditions close to the critical point, the asymptotic solutions show that this effect exhibits two distinct regimes depending on the initial distance to the critical point. One, not too close to the critical point, is the classical regime of the piston effect, known for a decade now and leading to a critical speeding up of the temperature relaxation; the other, closer to the critical point, is a regime where the piston effect is weakened by the diverging bulk viscosity, thus leading to a critical slowing down of the temperature relaxation. In the present analysis, the typical time scales of both regimes have been found explicitly, and a general solution describing all regimes (including the transitional intermediate regime) has been obtained. This result demonstrates that the piston effect is not governed by a single typical time scale, as believed until now, but by two time scales, one of which is a function of the bulk viscosity. This observation has led to the proposal of an alternative experimental strategy for measuring the bulk viscosity close to the critical point.

ACKNOWLEDGMENTS

The authors feel extremely indebted to Fang Zhong from the Jet Propulsion Laboratory (NASA / California Institute of Technology, Pasadena) and Horst Meyer from Duke University (Durham, North Carolina) for their precious advice.

APPENDIX: ASYMPTOTIC ANALYSIS OF THE EQUATIONS

1. Calculation in the boundary layer

In the boundary layer, the physical quantities T^*, P^*, ρ^*, and U^* are asymptotically expanded in the following way:

$$T^* = 1 + \Delta T + a\tilde{T}(z^*,\tau^*) + o(a),$$

$$P^* = 1 + \Delta P + b\tilde{P}(z^*,\tau^*) + o(b),$$

$$\rho^* = 1 + c\tilde{\rho}(z^*,\tau^*) + o(c),$$

$$U^* = d\tilde{U}(z^*,\tau^*) + o(d). \quad \text{(A1)}$$

$\tilde{T}$, $\tilde{P}$, $\tilde{\rho}$, and $\tilde{U}$ are order 1 functions of z^* and τ^*, while a, b, c, and d are gauge functions. As already defined in Eq. (18), τ^* is related to t^* through

$$\tau^* = et^*,$$

while z^* is defined as [see Eq. (16)]

$$z^* = \frac{x^*}{\delta}.$$

a, b, c, d, e, and δ are thus asymptotic functions of ϵ and ΔT.

An asymptotic analysis of Eqs. (6a)–(6d) is then conducted for ΔT and ϵ going to zero, with ζ and z^* fixed. In order to do so, ΔT is expressed as a function of the control parameter ζ,

$$\Delta T = \zeta \epsilon^{2/\chi}. \quad \text{(A2)}$$

The above expansions are then introduced in the equations of the problem (stars have again been omitted).

Mass conservation (6a),

$$ec\tilde{\rho}_\tau + \frac{d}{\delta}\tilde{U}_z = 0,$$

which leads to

$$ec = \frac{d}{\delta},$$

$$\tilde{\rho}_\tau + \tilde{U}_z = 0.$$

Momentum equation (6b),

$$ed\tilde{U}_\tau = -\frac{Ab}{\delta}\zeta^{-\alpha}\epsilon^{-2(\alpha/\chi)}\tilde{P}_z + d\frac{\epsilon\eta_0}{\delta^2}\zeta^{-(\alpha/2)-x_{\eta_\beta}}\epsilon^{-(\alpha+2x_{\eta_\beta})/\chi}\tilde{U}_{zz}.$$

The unsteady velocity term is negligible [9], so that the momentum equation becomes

$$A\tilde{P}_z = \eta_0\zeta^{(\alpha/2)-x_{\eta_\beta}}\tilde{U}_{zz}$$

with

$$b = \frac{d}{\delta}\epsilon^{1+[(\alpha-2x_{\eta_\beta})/\chi]}.$$

Equation of energy (6c),

$$ea\tilde{T}_\tau = -\frac{dB}{\delta}\zeta^{\alpha}\epsilon^{2\alpha/\chi}\tilde{U}_z + \epsilon\frac{\gamma_0 a}{Pr_0\delta^2}\zeta^{(\alpha/2)-x_\lambda}\epsilon^{(\alpha-2x_\lambda)/\chi}\tilde{T}_{zz}.$$

The unsteady temperature term is negligible too [9], which leads to

$$-B\zeta^{(\alpha/2)+x_\lambda}\tilde{U}_z + \frac{\gamma_0}{Pr_0}\tilde{T}_{zz} = 0,$$

$$d = \frac{a}{\delta}\epsilon^{1-[(\alpha+2x_\lambda)/\chi]}.$$

Equation of state (6d),

$$\tilde{P} = C\tilde{T} + D\zeta^{\gamma}\tilde{\rho},$$

$$b = a = c\epsilon^{2(\gamma/\chi)}.$$

The boundary condition in temperature is

$$T(z=0,\tau) = 1 + \Delta T + \theta T_w(\tau),$$

hence

$$a = \theta,$$

$$\tilde{T}(z=0,\tau) = T_w(\tau).$$

From here, we can calculate the gauge functions,

$$a = b = \theta,$$

$$c = \theta \epsilon^{-2(\gamma/\chi)},$$

$$d = \theta \epsilon^{(x_{\eta_\beta} - \alpha - x_\lambda)/\chi},$$

$$e = \epsilon^{(\alpha + x_{\eta_\beta} - x_\lambda)/\chi},$$

$$\delta = \epsilon^{1 - [(x_{\eta_\beta} + x_\lambda)/\chi]}.$$

The equations in the boundary layer can then be summarized (omitting the stars),

$$\tilde{\rho}_\tau + \tilde{U}_z = 0,$$

$$A\tilde{P}_z = \eta_0 \zeta^{(\alpha/2) - x_{\eta_\beta}} \tilde{U}_{zz},$$

$$-B\zeta^{(\alpha/2) + x_\lambda} \tilde{U}_z + \frac{\gamma_0}{Pr_0} \tilde{T}_{zz} = 0,$$

$$\tilde{P} = C\tilde{T} + D\zeta^\gamma \tilde{\rho}, \tag{A3}$$

with the boundary and initial conditions,

$$\tilde{T}(z=0,\tau) = T_w(\tau), \quad \tilde{U}(z=0,\tau) = 0,$$

$$\tilde{\rho}(z,\tau=0) = \tilde{P}(z,\tau=0) = \tilde{T}(z,\tau=0) = \tilde{U}(z,\tau=0) = 0.$$

Applying the Laplace transform to the above system (A3) and its boundary conditions, one finds

$$s\tilde{\rho} + \tilde{U}_z = 0,$$

$$A\tilde{P}_z = \eta_0 \zeta^{(\alpha/2) - x_{\eta_\beta}} \tilde{U}_{zz},$$

$$-B\zeta^{(\alpha/2) + x_\lambda} \tilde{U}_z + \frac{\gamma_0}{Pr_0} \tilde{T}_{zz} = 0,$$

$$\tilde{P} = C\tilde{T} + D\zeta^\gamma \tilde{\rho}, \tag{A4}$$

with

$$\tilde{T}(z=0,s) = T_w(s),$$

$$\tilde{U}(z=o,s) = 0.$$

The last system (A4) can be partially solved, with the following solutions:

$$\tilde{\rho} = K_0 \exp[-\sqrt{E(s)}z],$$

$$\tilde{U} = \frac{sK_0}{\sqrt{E(s)}} \{\exp[-\sqrt{E(s)}z] - 1\},$$

$$\tilde{T} = -\frac{K_0 B Pr_0}{\gamma_0} \zeta^{(\alpha/2) + x_\lambda} \frac{s}{E(s)} \{\exp[-\sqrt{E(s)}z] - 1\} + T_w(s), \tag{A5}$$

where $E(s)$ is given by

$$\frac{Pr_0 \zeta^{(\alpha/2) + x_\lambda - \gamma} s}{\gamma_0 (AD + \eta_0 \zeta^{(\alpha/2) - \gamma - x_{\eta_\beta}} s)} \tag{A6}$$

and K_0 is an integration constant, to be determined through the asymptotic matching with the bulk solutions.

2. Calculation in the bulk fluid

In the same way as in the boundary layer, T^*, P^*, ρ^*, and U^* are asymptotically expanded,

$$T^* = 1 + \Delta T + a\bar{T}(x^*, \tau^*) + o(a),$$

$$P^* = 1 + \Delta P + b\bar{P}(x^*, \tau^*) + o(b),$$

$$\rho^* = 1 + c\bar{\rho}(x^*, \tau^*) + o(c),$$

$$U^* = d\bar{U}(x^*, \tau^*) + o(d). \tag{A7}$$

$\bar{T}$, $\bar{P}$, $\bar{\rho}$, and $\bar{U}$ are order 1 functions of x^* and τ^*, while a, b, c, and d are again the related gauge functions (note that the same notations have been used as in the boundary layer, although the gauge functions in the bulk may be different from those in the boundary layer). An asymptotic analysis of Eqs. (6a)–(6d) is then conducted for ΔT and ϵ going to zero, with ζ and x^* fixed.

The matching condition between the velocity in the boundary layer and the bulk fluid is written (stars have again been omitted)

$$\theta \epsilon^{(x_{\eta_\beta} - \alpha - x_\lambda)/\chi} \tilde{U}(z \to \infty) = d\bar{U}(x=0),$$

which leads to

$$d = \theta \epsilon^{(x_{\eta_\beta} - \alpha - x_\lambda)/\chi},$$

$$\tilde{U}(z \to \infty) = \bar{U}(x=0).$$

In the same way, the matching condition between the bulk and boundary layer temperatures reads

$$\theta \tilde{T}(z \to \infty) = a\bar{T}(x=0),$$

which leads to

$$a = \theta,$$

$$\tilde{T}(z \to \infty) = \bar{T}(x=0).$$

The equation of mass conservation (6a) then becomes

$$c\epsilon^{(\alpha + x_{\eta_\beta} - x_\lambda)/\chi} \bar{\rho}_\tau + \theta \epsilon^{(x_{\eta_\beta} - \alpha - x_\lambda)/\chi} \bar{U}_x = 0,$$

from which one finds

$$c = \theta \epsilon^{-2/\chi},$$

$$\bar{\rho}_\tau + \theta \bar{U}_x = 0.$$

In the bulk equation of energy, the heat diffusion term is now negligible and the equation reads

$$ae\bar{T}_\tau = -B\zeta^\alpha \epsilon^{2\alpha/\chi} d\bar{U}_x,$$

which leads to

$$\bar{T}_\tau = -B\zeta^\alpha \bar{U}_x.$$

The equation of state can then be written

$$b\bar{P} = \theta C\bar{T} + D\theta\zeta^\gamma \epsilon 2\frac{\gamma-\alpha-x_\lambda}{\chi}\bar{\rho}.$$

From this is obtained

$$b = \theta,$$

$$\bar{P} = C\bar{T}.$$

Finally, the momentum equation becomes

$$\bar{P}_x = 0.$$

The equations of the problem in the bulk are summarized,

$$\bar{\rho}_\tau + \bar{U}_x = 0,$$

$$\bar{P}_x = 0,$$

$$\bar{T}_\tau = -B\zeta^\alpha \bar{U}_x,$$

$$\bar{P} = C\bar{T}, \tag{A8}$$

with the boundary and initial conditions,

$$\bar{U}(x=0) = \lim_{z\to\infty}\tilde{U}(z), \quad \bar{T}(x=0) = \lim_{z\to\infty}\tilde{T}(z),$$

$$\bar{T}_x(x=1) = 0, \quad \bar{U}(x=1) = 0,$$

$$\bar{\rho}(x,\tau=0) = \bar{P}(x,\tau=0) = \bar{U}(x,\tau=0) = \bar{T}(x,\tau=0) = 0.$$

Applying the Laplace transform to the system (A8), the following solutions can be obtained:

$$K_0 = \frac{-\gamma_0 E(s)}{sBPr_0\zeta^{(\alpha/2)+x_\lambda} + \gamma_0\zeta^\alpha B\sqrt{E(s)}} T_w(s)$$

and

$$\bar{\rho} = T_w(s)\frac{\gamma_0\sqrt{E(s)}}{sBPr_0\zeta^{(\alpha/2)+x_\lambda} + \gamma_0 B\zeta^\alpha\sqrt{E(s)}},$$

$$\bar{T} = T_w(s)\frac{\gamma_0\sqrt{E(s)}}{\gamma_0\sqrt{E(s)} + Pr_0\zeta^{x_\lambda-(\alpha/2)}s},$$

$$\bar{U} = T_w(s)\frac{\gamma_0 s\sqrt{E(s)}}{sBPr_0\zeta^{(\alpha/2)+x_\lambda} + \gamma_0 B\zeta^\alpha\sqrt{E(s)}}(1-x),$$

$$\bar{P} = T_w(s)\frac{C\gamma_0\sqrt{E(s)}}{\gamma_0\sqrt{E(s)} + Pr_0\zeta^{x_\lambda-(\alpha/2)}s}. \tag{A9}$$

The Laplace transforms of all the solutions in the bulk and boundary layer have thus been found in an explicit way. Note that in the above Laplace transforms, the Laplace parameter s is related to the dimensionless time variable τ^*.

3. Solutions of the problem at dimensional time t

The previous dimensionless solutions on the $\tau*$ time scale can now be rewritten as functions of the dimensional time variable t.

According to the properties of Laplace transforms, when two time variables τ^* and t are related by $\tau^* = \Omega t$, the corresponding Laplace variables s_{τ^*} and s_t are related by

$$s_{\tau^*} = \frac{1}{\Omega}s_t. \tag{A10}$$

For a function $f(\tau^*)$, the corresponding Laplace transforms $F(s_{\tau^*})$ and $\hat{F}(s_t)$ are related through

$$\hat{F}(s_t) = \frac{1}{\Omega}F\left(\frac{1}{\Omega}s_t\right). \tag{A11}$$

Here, $\tau^* = (eC_s/L)t$, with

$$e = \epsilon^{(\alpha+x_{\eta_\beta}-x_\lambda)/\chi}.$$

Then, $T_w(s_t) = (L/eC_s)T_w(s_{\tau^*})$. Therefore, the Laplace transform of the dimensional solutions is as follows.

In the boundary layer,

$$\tilde{\rho}(s) = -\frac{1}{B}T_w(s)\frac{\gamma_0 E(s)}{sPr_0\frac{L}{eC_s}\zeta^{(\alpha/2)+x_\lambda} + \gamma_0\zeta^\alpha\sqrt{E(s)}}\exp[-\sqrt{E(s)}z],$$

$$\tilde{T}(s) = -T_w(s)\frac{s}{s + \frac{eC\gamma_0}{LPr_0}\zeta^{(\alpha/2)-x_\lambda}\sqrt{E(s)}}\{1-\exp[-\sqrt{E(s)}z]\} + T_w(s),$$

$$\tilde{U}(s) = \frac{1}{B}T_w(s)\frac{s\gamma_0\sqrt{E(s)}}{sPr_0\zeta^{x_\lambda+(\alpha/2)} + \frac{eC_s\gamma_0}{L}\zeta^\alpha\sqrt{E(s)}} \times\{1-\exp[-\sqrt{E(s)}z]\},$$

$$\tilde{P}(s) = -CT_w(s)\frac{s}{s + \frac{eC_s\gamma_0}{LPr_0}\zeta^{(\alpha/2)-x_\lambda}\sqrt{E(s)}}\{1-\exp[-\sqrt{E(s)}z]\} - \frac{D}{B}\epsilon^{-2\gamma/\chi}T_w(s)\frac{\gamma_0 E(s)}{sPr_0\frac{L}{eC_s}\zeta^{(\alpha/2)+x_\lambda-\gamma} + \gamma_0\zeta^{\alpha-\gamma}\sqrt{E(s)}} \times\exp[-\sqrt{E(s)}z] + CT_w(s).$$

In the bulk,

$$\bar{\rho}(s) = \frac{1}{B}T_w(s)\frac{\gamma_0\sqrt{E(s)}}{\gamma_0\zeta^\alpha\sqrt{E(s)} + \frac{LPr_0}{eC_s}\zeta^{x_\lambda+(\alpha/2)}s},$$

$$\bar{T}(s) = T_w(s)\frac{\gamma_0\sqrt{E(s)}}{\gamma_0\sqrt{E(s)} + \frac{LPr_0}{eC_s}\zeta^{x_\lambda-(\alpha/2)}s},$$

$$\bar{U}(s) = \frac{1}{B}T_w(s)\frac{\gamma_0 s\sqrt{E(s)}}{\gamma_0\frac{eC_s}{L}\zeta^{\alpha}\sqrt{E(s)} + Pr_0\zeta^{x_\lambda+(\alpha/2)}s}(1-x),$$

$$\bar{P}(s) = CT_w(s)\frac{\gamma_0\sqrt{E(s)}}{\gamma_0\sqrt{E(s)} + \frac{LPr_0}{eC_s}\zeta^{x_\lambda-(\alpha/2)}s}.$$

The temperature solution in the bulk can now be expressed,

$$\bar{T}(s) = T_w(s)\frac{1}{1 + \frac{LPr_0}{eC_s}\zeta^{x_\lambda-(\alpha/2)}\frac{s}{\gamma_0\sqrt{E(s)}}}.$$

Replacing $E(s)$ by its expression and using $e=\epsilon^{(\alpha+x_{\eta_\beta}-x_\lambda)/\chi}$ and $\zeta=\Delta T\epsilon^{-2/\chi}$ leads to the result presented in Eq. (20).

[1] D. Dahl and M. R. Moldover, Phys. Rev. A **6**, 1915 (1972).
[2] J. Straub, L. Eicher, and A. Haupt, Phys. Rev. E **51**, 5556 (1995).
[3] A. Onuki, H. Hao, and R. A. Ferrell, Phys. Rev. A **41**, 2256 (1990).
[4] H. Boukari, J. N. Shaumeyer, M. E. Briggs, and R. W. Gammon, Phys. Rev. A **41**, 2260 (1990).
[5] B. Zappoli, D. Bailly, Y. Garrabos, B. Le Neindre, P. Guenoun, and D. Beysens, Phys. Rev. A **41**, 2264 (1990).
[6] L. P. Kadanoff and J. Swift, Phys. Rev. **166**, 89 (1968).
[7] K. Kawasaki, Phys. Rev. A **1**, 1750 (1970).
[8] A. Onuki, Phys. Rev. E **55**, 403 (1997).
[9] P. Carlès, Phys. Fluids **10**, 2164 (1998).
[10] K. A. Gillis, I. I Shinder, and M. R. Moldover, Phys. Rev. E **70**, 021201 (2004).
[11] P. Carlès, Ph.D. thesis, INPT, France (1995).
[12] Y. Garrabos, M. Bonetti, D. Beysens, F. Perrot, T. Frölich, P. Carlès, and B. Zappoli, Phys. Rev. E **57**, 5665 (1998).
[13] L. El Khouri, Ph.D. thesis, University Paris 6, France (2003).
[14] H. E. Stanley, *Introduction to Phase Transitions and Critical Phenomena* (Oxford University Press, New York, 1971).
[15] B. Quentrec, J. Phys. (Paris), Lett. **40**, 257 (1979).
[16] B. Zappoli and P. Carlès, Eur. J. Mech. B/Fluids **14**, 41 (1995).
[17] J. Kevorkian and J. D. Cole, *Perturbation Methods in Applied Mathematics* (Springer-Verlag, Berlin, 1981).
[18] F. Zhong (private communication).
[19] F. Zhong, A. Kogan, and H. Meyer, J. Low Temp. Phys. **108**, 161 (1997).
[20] R. F. Berg, M. R. Moldover, and G. A. Zimmerli, Phys. Rev. E **60**, 4079 (1999).
[21] F. Zhong and M. Barmatz (private communication).